rab4 Function in Membrane Recycling from Early Endosomes Depends on a Membrane to Cytoplasm Cycle*

Karin Mohrmann, Lisya Gerez, Viola Oorschot, Judith Klumperman, and Peter van der Sluijs‡

*From the Department of Cell Biology, University Medical Center Utrecht and Institute of Biomembranes,
Utrecht 3584 CX, The Netherlands*

The monomeric GTPase rab4 is associated with early endosomes and regulates recycling vesicle formation. Because the function of rab proteins in the biosynthetic pathway does not appear to depend on cycling between membranes and cytosol, we were interested to investigate whether or not this holds true for rab function in the endocytic pathway. We created a chimeric rab4 protein (NHrab4cbvn) in which the carboxyl-terminal prenylation motif was replaced by the transmembrane domain of cellubrevin. The chimeric protein was permanently attached to membranes, properly targeted to early endosomes, and bound guanine nucleotide to the same extent as wild type rab4. However, in transport assays we found that basolaterally endocytosed transferrin was less efficiently transported to the apical cell surface in Madin-Darby canine kidney cells transfected with NHrab4cbvn than in cells expressing wild type rab4. Hence, rab4 function requires ongoing cycles of association and dissociation from early endosomes. This cycle is altered during mitosis when rab4 accumulates in the cytoplasm through phosphorylation by a mitotic kinase. We show here, using a rab4 construct that is permanently hooked onto membranes, that the membrane-bound pool of rab4 is targeted by a mitotic kinase.

Small GTPases of the rab family are key regulators of vesicular transport in eukaryotic cells. More than 60 rab proteins have been identified, many of which are localized to intracellular organelles of the central vacuolar system (see Refs. 1 and 2). The active GTP-bound form of rab proteins associates with multiple other proteins, which may serve to relay the GTPase switch to effector systems such as SNARE[1] complexes involved in membrane docking and fusion (see Refs. 1 and 3) and the cytoskeleton for the coordination of organelle motility (4–6). It is thought that rab proteins may work as timers whose set point is determined by the relative rates of GTP hydrolysis and GDP exchange (7). rab GTPases cycle on and off membranes through the activity of a protein known as GDP dissociation inhibitor (GDI). GDI extracts the GDP form of rab proteins from membrane, shields their lipophilic carboxyl terminus from the aqueous cytoplasm, and can present complexed rab protein again to a donor membrane for a new activity cycle (see Ref. 8). The significance of a membrane to cytoplasm cycle for rab activity in the biosynthetic pathway has been called into question recently. Evidence for this notion derives from studies with Ypt1p chimeras in which the hydrophobic tails of the v-SNAREs Sec22p and Snc2p replaced the Ypt1p carboxyl terminus. These chimeric proteins appear to be correctly targeted and retain the function of Ypt1p in the biosynthetic pathway (9), although they are resistant to GDI extraction (10).

We have been investigating the role of rab4 in transport through the early endocytic pathway. rab4 regulates recycling from early endosomes (11–13) and is localized to vacuolar and tubular subdomains of early endocytic compartments and transport vesicles but not to the plasma membrane (13–15). rab4 is phosphorylated on Ser-196 during mitosis (16, 17). This increases the cytoplasmic pool ~5–10-fold, possibly due to the interaction with the mitotic peptidyl-prolyl isomerase Pin1 (18). Surprisingly, these phosphorylated rab4 molecules are in the GTP form. Because the cytoplasmic pool of rab proteins is thought to be in the GDP-bound form, this suggests that the additional rab4 molecules in the cytoplasm of mitotic cells are dissociated from early endosomes. Perturbation of the normal rab4 cycle by phosphorylation of either the cytoplasmic or membrane-bound pools may result in an increased cytoplasmic steady-state localization during mitosis. Hence, it has been difficult to establish whether membrane-bound rab4 is a target for mitotic kinases. To address this question, and to investigate whether membrane transport through early endosomes depends on cycles of rab4 dissociation and association with early endosomes, we constructed NHrab4cbvn in which we replaced the carboxyl-terminal Cys-Gly-Cys motif of rab4 with the transmembrane domain of cellubrevin, an endosomal v-SNARE. We found that NHrab4cbvn was fixed permanently on endosomal membranes and did not support rab4 function in membrane transport. The chimeric protein was phosphorylated during mitosis, showing that membrane-bound rab4 is targeted by mitotic kinases.

MATERIALS AND METHODS

Plasmid Construction and Antibodies—NHrab4pCB6 was described before (19). Mycrab4S196Q encodes rab4S196Q with an amino-terminal myc tag and was made with PCR using rab4S196QBSKS as template (17). Mycrab4S196Q was cloned into the *Eco*RI site of pCB6 to generate mycrab4pCB6. The NHrab4cellubrevin chimera consists of NHrab4 in which the carboxyl-terminal prenylation motif CGC was replaced by the putative transmembrane domain of cellubrevin. This construct was generated by overlap extension PCR using NHrab4 and cellubrevin

‡ To whom correspondence should be addressed: University Medical Center Utrecht, Dept. of Cell Biology, AZU Rm. G02.525, Heidelberglaan 100, Utrecht 3584 CX, The Netherlands. Tel.: 31-302-507-574; Fax: 31-302-541-797; E-mail: pvander@knoware.nl.

[1] The abbreviations used are: SNARE, soluble NSF attachment protein receptor; v-SNARE, vesicle-soluble NSF attachment protein receptor; NH, X31 influenza hemagglutinin; MDCK, Madin-Darby canine kidney; CHO, Chinese hamster ovary; Tf, transferrin; mychTfR, Myc-tagged human transferrin receptor; PNS, post nuclear supernatant; cbvn, cellubrevin; MCFM, methionine/cysteine-free medium; PFM, phosphate-free medium; GDI, GDP dissociation inhibitor; MEM, modified Eagle's medium; PBS, phosphate-buffered saline; MES, 4-morpholineethanesulfonic acid; ER, endoplasmic reticulum.
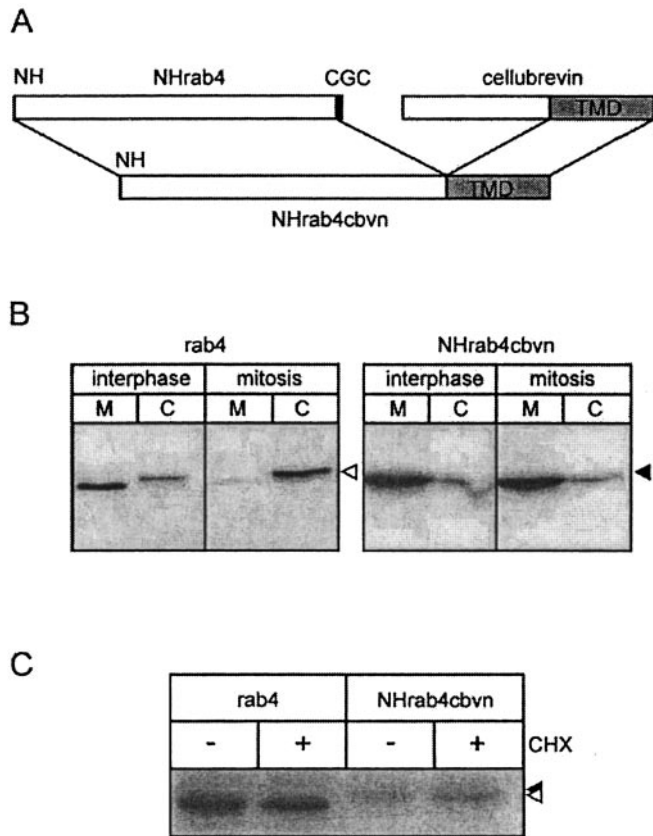
FIG. 1. **NHrab4cbvn is bound to membranes and phosphorylated during mitosis.** *A*, the domain structure of NHrab4cbvn, consisting of NH-tagged rab4, in which the carboxyl-terminal Cys-Gly-Cys motif has been replaced by the membrane anchor of cellubrevin. Interphase and mitotic NHrab4cbvnCHO cells were fractionated by ultracentrifugation. NHrab4cbvn was analyzed by Western blotting in PNS, membrane (*M*), and cytosol (*C*) fractions using a rabbit antibody against rab4. Note that NHrab4cbvn cofractionated with membranes during interphase and mitosis (*B*). Mitotic rab4CHO and NHrab4cbvnCHO cells were metabolically labeled with [^{32}P]orthophosphate for 45 min in the absence or presence of cycloheximide. Cells were lysed in detergent. rab4 was immunoprecipitated from cleared detergent lysates and analyzed by SDS-PAGE and phosphorimaging. *Open* and *closed arrowheads* mark rab4 and NHrab4cbvn, respectively (*C*).

FIG. 2. **Guanine nucleotide binding of NHrab4cbvn.** Interphase rab4CHO and NHrab4cbvnCHO cells were metabolically labeled for 2 h with 175 μCi/ml [^{32}P]orthophosphate and lysed as described under "Materials and Methods." The protein content of lysates was determined by the bis-cinchonic acid method. Mutant and wild type rab4 were immunoprecipitated from equal amounts of detergent lysates with a polyclonal rab4 antibody that does not detect endogenous rab4 by immunoprecipitation (18). Guanine nucleotides were eluted from immunoprecipitates, resolved by TLC, and analyzed by phosphorimaging. The figure shows a representative result from at least three independent experiments. Quantitation was done with the ImageQuaNT software package.

tants were synchronized in prometaphase as described (18). The cells were washed once with phosphate-free MEM (Sigma Chemical Co., St Louis, MO) containing 40 ng/ml nocodazole, starved for 30 min at 37 °C in nocodazole, and labeled for 45 min with 175 μCi/ml [^{32}P]orthophosphate in the absence or presence of 10 μg/ml cycloheximide. The cells were then lysed in 1% Triton X-100, 10 mM sodium fluoride, 25 mM sodium β-glycerophosphate, 1 mM sodium vanadate, 1 mM phenylmethylsulfonyl Fluoride in PBS, and rab4 was immunoprecipitated from detergent lysates as described (25). For determination of guanine nucleotide ratios in interphase cells, cells were labeled for 2 h with [^{32}P]orthophosphate as described above (in the absence of nocodazole). Bound GDP and GTP were analyzed by thin layer chromatography (TLC) of immunoprecipitates precisely as done before (18).

Pulse-Chase Experiments—Transfectants were washed once with methionine and cysteine free MEM (Sigma, St. Louis, MO) (MCFM) and incubated for 30 min at 37 °C in MCFM. Next, the cells were labeled for 30 min with 0.2 mCi/ml Tran^{35}S-label in MCFM and chased for different periods of time in αMEM containing 10% fetal calf serum, 5 mM cysteine, and 5 mM methionine. Cells were lysed in PBS containing 1% Triton X-100, 1 mM phenylmethylsulfonyl fluoride, 10 μg/ml aprotinin, 5 μg/ml leupeptin, 10 μg/ml pepstatin, and centrifuged for 10 min at 15,000 rpm at 4 °C. rab4 and NHrabvcbvn were immunoprecipitated from the supernatant as described (18), and analyzed by SDS-PAGE.

Subcellular Fractionation—CHO transfectants were washed once with ice-cold medium and once with 250 mM sucrose, 1 mM EDTA, 1 mM phenylmethylsulfonyl fluoride, 3 mM imidazole, pH 7.4. Cells were resuspended in 0.5 ml of homogenization buffer and broken by passing them through a 25-gauge needle. Post nuclear supernatants (PNS) were prepared by centrifugation of homogenates for 15 min at 3500 rpm at 4 °C. High speed supernatants and membrane pellets were obtained by centrifugation of PNS at 150,000 $\times$ *g* for 1 h at 4 °C in a TLS55 rotor. Membrane fractions enriched in early and late endosomes were resolved on discontinuous sucrose gradients in an SW60 rotor as described previously (26).

Recycling of [^{125}I]Tf—Human Tf was saturated with Fe^{3+} (11), and iodinated as described (27). MDCK transfectants were grown on 24 mm Transwell filters and depleted of endogenous Tf during a 60 min incubation in MEM, 20 mM HEPES pH 7.4, 0.1% BSA, 50 μM Deferoxamine (medium), and depleted from endogenous transferrin for 60 min at 37 °C. [^{125}I]Tf (2 μg/ml) was internalized basolaterally for 30 min in 1 ml of medium without deferoxamine at 16 °C. The cells were transferred to ice, washed twice with PBS, once with MES buffer (20 mM MES, pH 5.0, 130 mM NaCl, 2 mM CaCl$_2$, 0.1% bovine serum albumin, 50 mM deferoxamine), and once with PBS (each 10 min). The acid-neutral-wash cycle was repeated once, and the cells were then chased in

(generously provided by Thomas Südhof, Southwestern Medical Center, Dallas, TX) as templates and ligated between the *Kpn*I and *Bam*HI sites of pcDNA3 (Invitrogen, Leek, The Netherlands). Myc-tagged human transferrin receptor (mychTfR) cDNA was excised with *Sac*I and *Xba*I from mychTfR-pCB6 and ligated in pCB7 (generously provided by Jim Casanova, Harvard Medical School, Boston, MA). cDNAs created by the polymerase chain reaction were verified by dideoxy sequencing. The rabbit antibody MC16 against the amino terminus of cellubrevin (20) was generously provided by Thierry Galli (Institute Curie, Paris). Rabbit antibodies against rab4 (21) and the antibodies against the X31 influenza hemagglutinin NH epitope (19), the myc epitope (22), and tubulin (23) were described before. Labeled secondary antibodies were from Molecular Probes (Leiden, The Netherlands) and Jackson ImmunoResearch Laboratories (Westgrove, PA).

Cell Culture, Transfection, and Synchronization—CHO cells and rab4CHO cells have been described previously (11). CHO cells were stably transfected with mycrab4S196QpCB6 or NHrab4cbvnpcDNA3 and grown as before (24). MDCKII cells were grown in MEM (Invitrogen, Breda, The Netherlands) containing 10% fetal calf serum, 100 units/ml penicillin, and 100 μg/ml streptomycin. To facilitate the analysis of Tf kinetics, we generated a stable mychTfRMDCKII cell line by transfecting MDCKII cells with mychTfRpCB7. These cells were grown in media containing 200 units/ml hygromycin. mychTfRMDCKII cells were double-transfected with NHrab4cbvnpcDNA3 or rab4pcDNA3 and maintained in media containing 0.6 mg/ml G418 and 200 units/ml hygromycin. The cells received 5 mM sodium butyrate 18 h prior to experiments to induce expression of cytomegalovirus-driven constructs.

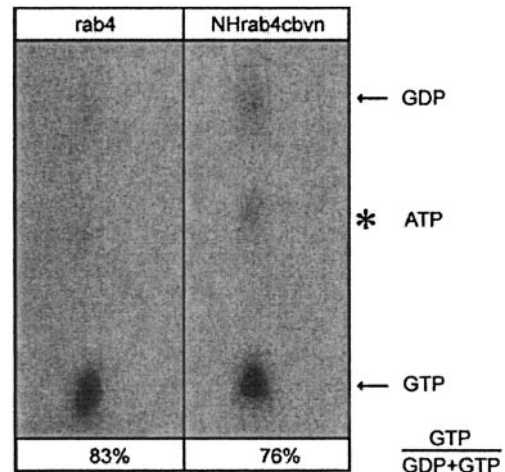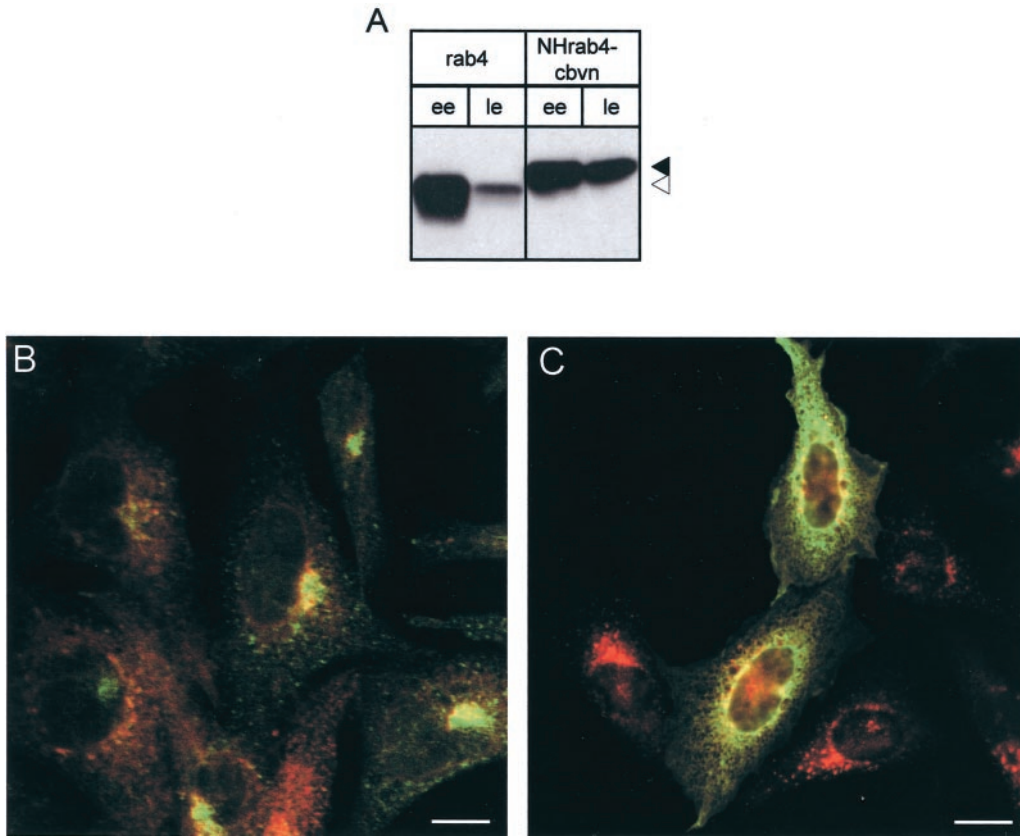*In Vivo Phosphorylation and Immunoprecipitation*—CHO transfec-

FIG. 3. **Confocal immunofluorescence microscopy.** *A*, interphase rab4CHO and NHrab4cbvnCHO were homogenized, and PNS was resolved by discontinuous sucrose gradient centrifugation in membrane fractions enriched in early endosomes (*ee*) and late endosomes (*le*). The presence of rab4 and NHrab4cbvn was assayed by Western blotting using a rab4 antibody. *Open* and *closed arrowheads* denote the positions of rab4 and NHrab4cbvn, respectively. *B*, double-label confocal immunofluorescence microscopy of NHrab4cbvnCHO cells in which endogenous cellubrevin (*green*) was labeled with a rabbit antibody against an amino-terminal epitope, and NHrab4cbvn (*red*) with a monoclonal antibody against the NH epitope tag. The *red* and *green images* were separately scanned and subsequently merged to emphasize the areas of overlapping distribution, which appear as *yellow*. *C*, double-label confocal immunofluorescence microscopy of the NHrab4cbvn/mycrab4S196QCHO double transfectant. NHrab4cbvn (*green*) was detected with a rabbit antibody against the NH epitope tag, whereas mycrab4S196Q (*red*) was detected with the monoclonal antibody 9E10 against myc. *Scale bars*, 20 μm.

prewarmed medium at 37 °C. Chase media were collected after different periods of time, and the cells were washed twice with ice-cold medium. [^{125}I]Tf in media and cells was established in a γ-counter, and the results are expressed as the percentage of total in media and on filters.

Immunoelectron Microscopy—rab4CHO cells and NHrab4cbvnCHO cells were fixed for immunoelectron microscopy with a mixture of 2% freshly prepared formaldehyde and 0.2% glutaraldehyde in 0.1 M phosphate buffer, pH 7.4. After 6 h at room temperature the fixative was replaced and cells were post-fixed in 2% formaldehyde overnight at 4 °C. Cells were then prepared for Ultrathin cryosectioning and immunogold labeled according to the protein A-gold method as previously described (28, 29). Briefly, fixed cells were washed once in PBS with 0.02 M glycine, after which cells were scraped in 1% gelatin in PBS and embedded in a 12% gelatin solution. The cell-gelatin mixture was solidified on ice and cut into small blocks. After infiltration with 2.3 M sucrose at 4 °C, blocks were mounted on aluminum pins and frozen in liquid nitrogen. Ultrathin cryosections were picked up in a mixture of 50% sucrose/50% methyl cellulose, which improves preservation of the ultrastructure (30). Sections were labeled with a polyclonal antibody against rab4 (21), which was previously used for the ultrastructural localization of rab4 in PC12 cells (13, 15).

Miscellaneous Methods—Immunofluorescence microscopy, isolation of prometaphase cells, and Western blot were done precisely as described (18, 25, 31).

RESULTS

NHrab4cbvn Is Constitutively Associated with Membranes during the Cell Cycle—rab4 cycles between a membrane-bound state and a cytosolic form that is complexed with GDI (32), whereas the association of rab4 with endosomes depends on the

presence of a carboxyl-terminal Cys-Gly-Cys prenylation motif (17). However, the function of this cycle in the control of membrane transport through early endosomes is incompletely understood. We therefore constructed an epitope-tagged rab4 chimera in which the Cys-Gly-Cys was replaced with the putative transmembrane anchor of the endosomal v-SNARE, cellubrevin. A schematic of the chimera's domain structure is shown in Fig. 1*A*. We stably transfected the construct into CHO cells and investigated its distribution over membranes and cytosol using high speed centrifugation. As we previously showed for wild type rab4, the NHrab4cbvn chimera was mainly in the membrane fraction of interphase cells. In contrast to wild type rab4, which is predominantly localized in the cytoplasm during mitosis, NHrab4cbvn remained associated with membranes (Fig. 1*B*) in dividing cells. These results show that replacement of the carboxyl-terminal prenylation motif with the hydrophobic transmembrane domain of cellubrevin fixed rab4 permanently on membranes.

We next investigated whether membrane-associated NHrab4-cbvn is phosphorylated by a mitotic kinase during cell division. For this purpose, mitotic cells expressing wild type rab4 or NHrab4cbvn were labeled with [^{32}P]orthophosphate. Proteins were then immunoprecipitated from detergent lysates with a rab4 antibody and analyzed by SDS-PAGE. As shown in Fig. 1*C*, NHrab4cbvn became phosphorylated during mitosis, albeit to a lesser extent than wild type rab4. Because the chimeric protein contains the NH epitope tag and cellubrevin membrane
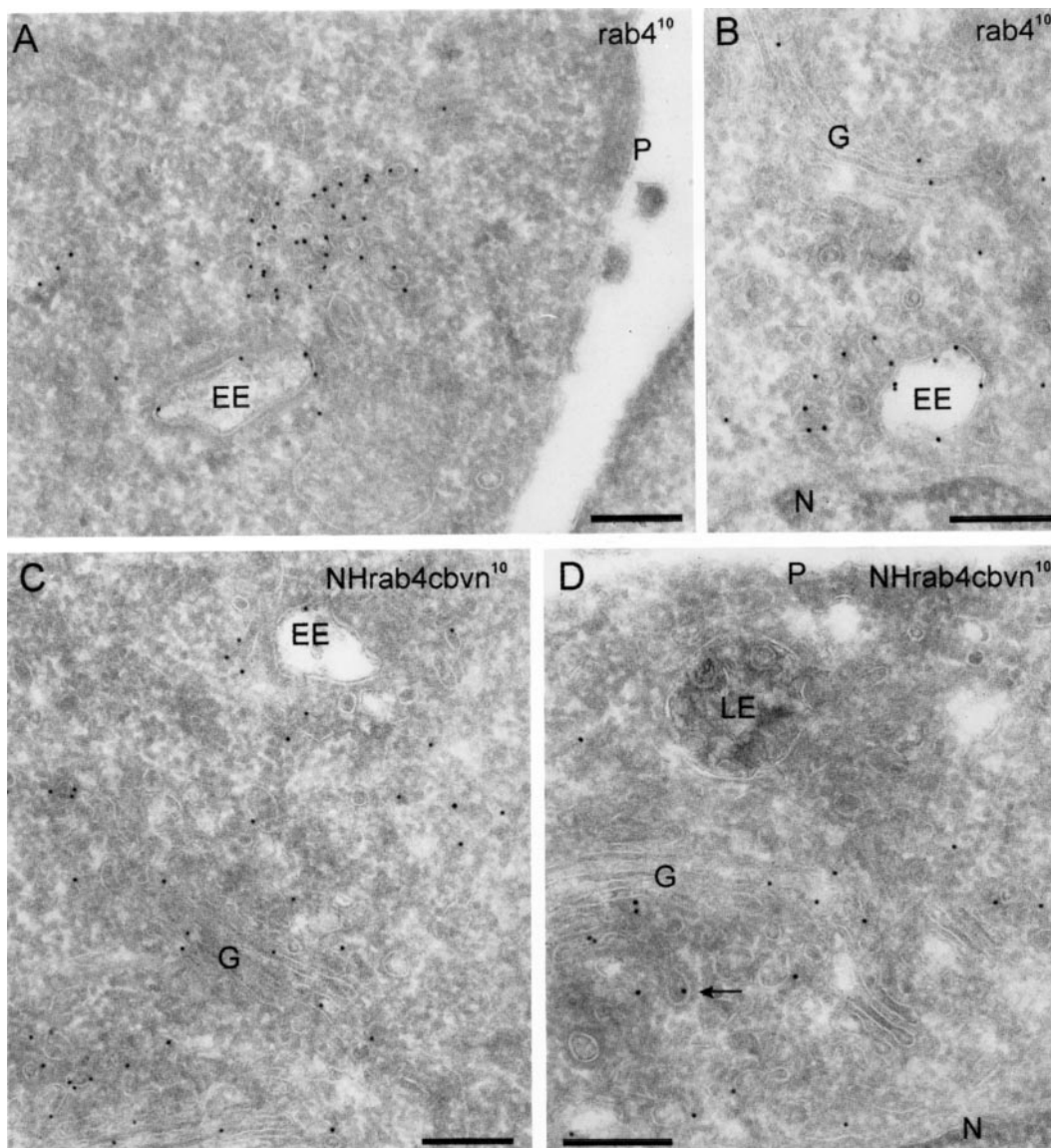
FIG. 4. **Ultrastructural localization of rab4 and NHrab4cbvn.** Ultrathin cryosections were labeled with polyclonal anti-rab4 and protein A conjugated to 10-nm gold. *A*, in wild type rab4 cells the majority of 10-nm gold label is found in early endosomes (*EE*) and associated recycling vesicles. The plasma membrane (*P*) is devoid of label (*A*). An additional but small pool of wild type rab4 label is found in the Golgi (*G*) stack (*B*). NHrab4cbvn (10-nm gold) is also found in early endosomes (*EE*), whereas a sizeable fraction is in the Golgi stack and membranes in the Golgi area. Sometimes NHrab4cbvn is seen in clathrin-coated membranes (*arrow*), clearly indicating the trans side of the Golgi complex. Late endosomes (*LE*) and plasma membrane (*P*) are negative for the chimeric protein (*D*). *N*, nucleus. *Scale bars*, 200 nm.

anchor, its molecular mass increases 3 kDa, which reduced the electrophoretic mobility as compared with wild type rab4. Although the expression levels of rab4 and NHrab4cbvn were the same (not shown), we found a lower overall [^{32}P]orthophosphate incorporation as measured by trichloroacetic acid precipitation in the NHrab4cbvnCHO cell line than in rab4CHO cells. After correction for the different ^{32}P labeling efficiencies between the two cell lines, NHrab4cbvn was ~60% as efficiently phosphorylated as rab4. To exclude the possibility that the phosphorylated NHrab4cbvn band represented newly synthesized protein that was not yet associated with membranes, we repeated the experiment in the presence of the protein synthesis inhibitor cycloheximide. As shown in Fig. 1*C*, cycloheximide did not prevent phosphorylation of the chimeric protein. This documented that phosphorylation of the existing pool of membrane-associated NHrab4cbvn solely accounted for the band in Fig. 1*C*.

Guanine Nucleotide Binding of NHrab4cbvn—rab proteins cycle between an inactive GDP-bound form and an active GTP-

bound state. Delivery of a cytosolic rab in a GDP state from an rab·GDI complex is thought to be followed by activation through a guanine nucleotide exchange factor (33, 34). We were next interested to determine whether or not membrane-bound NHrab4cbvn might be targeted for GTP binding. Because a guanine nucleotide exchange protein for rab4 has not been identified yet, it was not possible to use a defined system for guanine nucleotide exchange assays. Instead, we determined the guanine nucleotide state of NHrab4cbvn *in vivo*, which reflects the net effect of ongoing GTP hydrolysis and GDP/GTP exchange. CHO cells expressing NHrab4cbvn were metabolically labeled with [^{32}P]orthophosphate, and guanine nucleotide content was determined by TLC of eluted immunoprecipitates. As shown in Fig. 2, NHrab4cbvn and rab4 had similar steady-state GTP/GDP ratios, suggesting that the mutant had the same guanine nucleotide binding properties as wild type rab4. To rule out that this was a cell type-specific result, we repeated the experiment in Madin-Darby canine kidney (MDCK) cells transfected with NHrab4cbvn or wild type rab4 and found
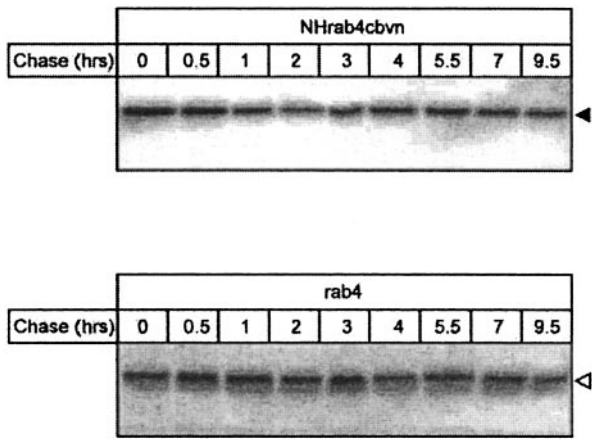
Fig. 5. **Stability of newly synthesized NHrab4cbvn.** Interphase rab4CHO and NHrab4cbvnCHO transfectants were labeled for 30 min with 200 μCi/ml Tran[35]S-label and chased for various periods of time. Cells were lysed at the end of the chase times, and rab4 was immunoprecipitated from detergent lysates. Immunoprecipitates were resolved by SDS-PAGE on 12.5% gels, and rab4 and NHrab4cbvn were detected by phosphorimaging. *Open* and *closed arrowheads* denote the positions of rab4 and NHrab4cbvn, respectively.

essentially the same result (not shown). Thus permanent attachment of rab4 to membranes did not compromise its ability to bind GTP and GDP.

NHrab4cbvn Is Associated with Early Endosomes—The availability of the chimeric protein also allowed us to investigate whether rab4 function critically relied on a membrane to cytoplasm cycle. We first biochemically analyzed whether NHrab4cbvn was targeted to early endosomes. NHrab4cbvnCHO transfectants were homogenized and postnuclear supernatants were fractionated using an established protocol to separate early and late endosome-enriched membranes (26). As shown in Fig. 3*A*, >60% of the NHrab4cbvn chimera was distributed in the high density interface representing early endocytic compartments. The amount of NHrab4cbvn in the low density sucrose interface most likely represented NHrab4cbvn molecules in biosynthetic compartments, because endoplasmic reticulum (ER) and Golgi membranes are known to cofractionate with late endosomes in these gradients (35). In a parallel gradient we analyzed the distribution of rab4 on membranes from rab4CHO cells. In these cells rab4 was almost exclusively distributed in the high density membrane fraction.

To define the localization of NHrab4cbvn by morphological methods, we first compared its distribution with that of cellubrevin and rab4 using confocal fluorescence microscopy and immunoelectron microscopy. For double-label experiments in which we wanted to establish the distribution of the chimera with respect to cellubrevin, we took advantage of the fact that the epitope of the MC16 antibody against cellubrevin is in the amino terminus of the protein (20). This domain of cellubrevin is not present in NHrab4cbvn (Fig. 1*A*). The chimera was detected with the monoclonal against the NH epitope tag. As shown in Fig. 3*B* and documented previously (24), endogenous cellubrevin (*green*) was present in a compact structure around the nucleus and in small peripheral punctae in the cytoplasm. The chimeric protein (*red*) codistributed with endogenous cellubrevin into this perinuclear compartment and localized to the ER/nuclear envelope. To analyze the distribution of NHrab4cbvn with respect to rab4, we transiently transfected mycS196Qrab4CHO cells with NHrab4cbvn cDNA. This rab4 mutant lacks the p34[cdc2] kinase phosphorylation site and has the same distribution as wild type rab4 in interphase cells (11,

17). Cells were stained with the monoclonal antibody 9E10 to detect mycS196Qrab4 and with a polyclonal antibody against the NH epitope tag to detect NHrab4cbvn. Fig. 3*C* shows a significant overlap in localization between mycS196Qrab4 (*red*) and NHrab4cbvn (*green*) on the nuclear envelope, in the perinuclear region, and in vesicular structures in the cytoplasm. This confirmed the results of Fig. 3*A*, in which a fraction of NHrab4cbvn was found in the region of the gradient to which the ER and Golgi sedimented. Because cellubrevin and rab4 have partially overlapping and distinct distributions (24), it was not surprising that NHrab4cbvn did not precisely colocalize on the same structures with these two proteins. We next compared its distribution with that of rab4 at the ultrastructural level using immunoelectron microscopy (Fig. 4). In rab4CHO cells, the 10-nm gold particles representing rab4 were predominantly found at early endosomes, especially at the associated recycling vesicles (Fig. 4*A*). Irrespective of expression levels (not shown), rab4 was always absent from the plasma membrane, whereas a small fraction (~6%) localized to the Golgi stack (Fig. 4*B*) as we showed before in PC12 cells (13, 15). In NHrab4cbvn cells, label was again found on early endosomes and associated vesicles (Fig. 4*C*) but less abundantly than wild type rab4 in the rab4 CHO cells as was already suggested by the subcellular fractionation and immunofluorescence data in Fig. 3. The labeling of the Golgi stack and associated vesicles, however, had markedly increased (Fig. 4, *C* and *D*), reflecting transport of the protein through the ER to Golgi pathway for biosynthesis. Late endosomes and plasma membrane were not labeled for the chimera (Fig. 4*C*) as was also found for with wild type rab4 (Fig. 4*B*). Although the immunofluorescence microscopy clearly documented detectable levels of NHrab4cbvn in the nuclear envelope and ER, on Ultrathin cryosections the level of immunoreactivity, representing protein concentration per membrane unit, was below the detection level in the elaborate meshwork of ER membranes as we noted before with other antigens (36).

Stability of NHrab4cbvn—Because we found a partial localization of NHrab4cbvn to the ER by immunofluorescence microscopy, we determined whether this represents a fraction of improperly folded newly synthesized protein that might be targeted for degradation. To investigate this question we determined the stability of NHrab4cbvn with respect to wild type rab4 using a pulse-chase approach. Cells were metabolically labeled for 30 min with Tran[35]S-label and chased for different periods of time in the absence of label, and NHrab4cbvn and rab4 were immunoprecipitated from detergent lysates. Even after 9.5 h of chase we did not find appreciable degradation of the chimeric protein or wild type rab4 as documented in Fig. 5. Extending chase times up to 24 h decreased viability of the cells, which caused a similar reduction of immunoprecipitable NHrab4cbvn and wild type rab4 (not shown). Thus NHrab4cbvn has the same turnover rate as wild type rab4 and is an intrinsically long-lived protein.

A Membrane-Cytoplasm Cycle Is Necessary for rab4 Function—Finally, we analyzed whether rab4 needs to cycle between membrane-bound and cytoplasmic pools to perform its function in regulating membrane recycling from early endosomes. To address this question we used filter-grown MDCK cells, a well characterized model system to investigate vesicular transport in polarized epithelial cells. MDCK cells recycle internalized Tf nearly quantitatively to the basolateral plasma membrane, and perturbation of Tf transport through early endosomes can be conveniently monitored by measuring enhanced transport of Tf into the apical medium (37, 38). To investigate the function of NHrab4cbvn, we generated stable MDCK double transfectants expressing mychTfR and

FIG. 6. **Functional characterization of NHrab4cbvn in MDCK transfectants.** Characterization of MDCK cells transfected with mychTfR (*1*), mychTfR and rab4 (*2*), or mychTfR and NHrab4cbvn (*3*). Cells were lysed in 1% TX-100, and the levels of mychTfR, rab4, and NHrab4cbvn were analyzed by Western blotting. The three cell lines expressed similar levels of mychTfR, whereas the rab4 constructs were expressed ~5–7 times above endogenous rab4. Tubulin served as loading control (*A*). MDCKII cells stably transfected with the mychTfR (control) or double-transfected with mychTfR and rab4 and NHrab4cbvn were grown on 24-mm Transwell filters for 4 days. Cells were loaded with [^{125}I]transferrin at 16 °C for 60 min from the basolateral side, washed, and chased at 37 °C. Apical and basolateral media were collected at different periods of time, and [^{125}I]Tf is expressed as the percentage of total. Data are means ± S.D. of three independent experiments (*B*).
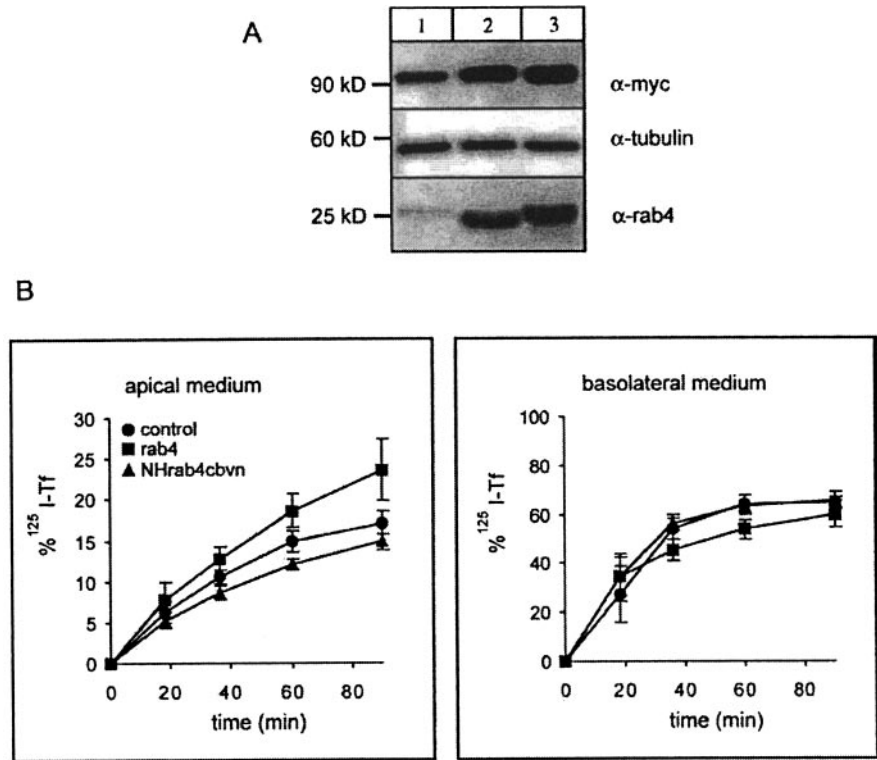
NHrab4cbvn, or mychTfR and rab4. As shown in Fig. 6*A*, the expression levels of rab4 and NHrab4cbvn were similar in these cell lines as was the case for mychTfR. Next we analyzed transport of [^{125}I]Tf in these cells. For this purpose, we internalized [^{125}I]Tf at 16 °C, to accumulate the tracer in basolateral early endosomes. After 60 min, the three cell lines contained the same amount of [^{125}I]Tf, suggesting that NHrab4cbvn did not effect internalization (not shown). The cells were then chased at 37 °C, and delivery of [^{125}I]Tf to the apical and basolateral media was determined. In this assay, the wild type rab4 transfectant showed increased transport of [^{125}I]Tf into the apical medium as compared with control MDCK cells not transfected with rab4 (Fig. 6*B*). In NHrab4cbvnMDCK cells, however, we observed the same transport kinetics of [^{125}I]Tf as in the control MDCK cells. We previously showed that wild type rab4 as well as the GTP hydrolysis-deficient rab4Q67L mutant enhanced apical delivery of basolaterally endocytosed Tf (38). In contrast, in cells expressing the inhibitory S22Nrab4, Tf was transported with the same kinetics as in mock transfected cells. The inhibitory phenotype of NHrab4cbvn, however, is mechanistically distinct from that of S22Nrab4, because the former occurs predominantly in the GTP-bound state (Fig. 2), whereas S22Nrab4 binds GDP to a limited extent but not GTP (18). Because the NHrab4cbvn chimera and S22Nrab4 reveal identical transport phenotypes, we conclude that the permanent attachment of rab4 to membranes generates an inactive rab4 mutant, unable to perform wild type rab4 function.

DISCUSSION

Protein phosphorylation plays a key role in the regulation of membrane transport and organelle inheritance during the mammalian cell cycle. Intracellular transport is coordinately inhibited in dividing cells, and organelle fragmentation is thought to occur due to ongoing transport vesicle formation while membrane fusion is inhibited. The molecular mechanisms underlying the inhibition of membrane transport during mitosis are only partially understood. rab4 regulates membrane transport through early endosomes and is phosphorylated by p34^{cdc2} kinase (11, 17). Thus rab4 is likely to be one of the targets for the inhibition of endocytic transport. Indeed, although rab4 is associated with endosomes in interphase, during mitosis it is localized to the cytoplasm in a complex with the peptidyl prolylisomerase Pin1 and presumably unable to perform its endosomal function (18). Why phosphorylated rab4 is localized to the cytoplasm is not clear. Phosphorylation of the cytoplasmic rab4 pool might inhibit its recruitment to endosomes. Alternatively, phosphorylation of membrane-bound rab4 may enhance its dissociation into the cytoplasm. Both scenarios or a combination thereof will result in the depletion of rab4 from early endosomes and the build-up of a cytoplasmic pool of rab4 molecules. A rab4 truncation mutant that is constitutively expressed in the cytoplasm does become phosphorylated during mitosis, which is consistent with a model in which phosphorylated cytoplasmic rab4 molecules fail to be recruited to endosomes (17). Informative as it is, this result cannot be used as evidence against the second model, because it is not known whether the endosomal pool of rab4 might be targeted by a mitotic kinase.

We addressed this question in expression experiments with an rab4 construct that was permanently attached to early endosomes, because its consensus sequence for carboxyl-terminal isoprenylation was replaced by the transmembrane domain of the endosomal v-SNARE, cellubrevin. The chimeric protein was membrane-associated in both interphase and mitotic cells. During mitosis NHrab4cbvn was phosphorylated, showing for the first time that phosphorylation of rab4 can also occur on membranes. This also explains the previous finding that phosphorylated cytoplasmic rab4 is in the GTP-bound form (18). Because rab4 guanine nucleotide exchange activity remains membrane-associated during mitosis (32), enhanced dissociation of phosphorylated rab4-GTP from endosomes increases the number of cytoplasmic rab4 molecules in the GTP-bound form.

GTP hydrolysis on rab proteins was initially thought to be required for membrane docking and fusion or recycling of the

GDP-bound form back to the donor organelle (39). More recent experiments with Ypt1p and Sec4p that were permanently attached to membranes have called this concept into question (9). These mutants appeared to be targeted to the correct membranes and reportedly retained the capacity to maintain vesicular transport through the biosynthetic pathway. In contrast to these rab proteins that act between the ER and the plasma membrane, our recycling experiments in MDCK cells, however, showed that NHrab4cbvn cannot substitute for wild type rab4.

Because rab proteins are important for tethering of transport vesicles to their target membrane (see Ref. 40) and for their formation at the donor compartment (13, 41–43), a salvage pathway is required to recycle rab proteins from the acceptor membrane. GDI-mediated extraction followed by cytosolic transfer of a rab·rab GDI complex back to the donor or transport vesicle is an attractive mechanism that is supported by experimental evidence, although it is also possible that retrieval to the donor membrane may occur via a retrograde transport pathway. The observation, that NHrab4cbvn permanently resides on membranes and has an inhibitory phenotype in the transport assay, suggests that a cycle of rab4 between membrane and cytosol is important for its function in membrane recycling from early endosomes. It is unlikely that retrieval of NHrab4cbvn to early endosomes proceeds via the cell surface and endocytosis, because immunoelectron microscopy shows that neither rab4 (13, 15) nor NHrab4cbvn localize to the plasma membrane.

Why would rab4 behave differently in this respect than do Ypt1p and Sec4p? At least two explanations can be put forward to account for this disparity. First, even though the biosynthetic and endocytic pathways are regulated by members of conserved protein families, there appear to be clear differences. For instance, deletion of the *YPT1* or *SEC4* genes in yeast is lethal (44, 45), whereas knockout strains of *YPT5*, whose product regulates the endocytic pathway, are viable (46). Second, because rab GTPases exert their functions in membrane transport through multiple effector proteins (reviewed in Ref. 1), this may simply indicate that there is not necessarily a common principle by which rab proteins control membrane traffic. An example of this idea is provided by rab27a, which in melanocytes cooperates with myosin Va (6, 47) but not in cytotoxic T lymphocytes (48). Presently, five rab4 effector proteins have been characterized. These are rabaptin-4 (49), rabaptin-5 (50), rabenosyn-5 (51), rabip4 (52), and the cytoplasmic dynein light intermediate chain-1 (53), the first three of which are bifunctional ones that also interact with rab5. Clearly a further understanding of membrane recycling via early endosomes requires the identification and characterization of additional rab4 effector and accessory proteins.

REFERENCES

1. Zerial, M., and McBride, H. (2001) *Nat. Rev. Mol. Cell. Biol.* **2,** 107–117
2. Pereira-Leal, J. B., and Seabra, M. C. (2000) *J. Mol. Biol.* **301,** 1077–1087
3. Chen, Y. A., and Scheller, R. H. (2001) *Nature Rev. Mol. Cell. Biol.* **2,** 98–106
4. Echard, A., Jollivet, F., Martinez, O., Lacapere, J. J., Rousselet, A., Janoueix-Lerosey, I., and Goud, B. (1998) *Science* **279,** 580–585
5. Nielsen, E., Severin, F., Backer, J. M., Hyman, A. A., and Zerial, M. (1999) *Nat. Cell Biol.* **1,** 376–382
6. Wu, X., Rao, K., Bowers, M. B., Copeland, N. G., Jenkins, N. A., and Hammer, J. A., III (2001) *J. Cell Sci.* **114,** 1091–1100
7. Rybin, V., Ullrich, O., Rubino, M., Alexandrov, K., Simon, I., Seabra, M., Goody, R., and Zerial, M. (1996) *Nature* **383,** 266–269
8. Pfeffer, S. R. (2001) *Trends Cell Biol.* **11,** 487–491
9. Ossig, R., Laufer, W., Schmitt, H. D., and Gallwitz, D. (1995) *EMBO J.* **14,** 3645–3653
10. Cao, X., and Barlowe, C. (2000) *J. Cell Biol.* **149,** 55–65
11. van der Sluijs, P., Hull, M., Webster, P., Goud, B., and Mellman, I. (1992) *Cell* **70,** 729–740
12. Roberts, M., Barry, S., Woods, A., van der Sluijs, P., and Norman, J. (2001) *Curr. Biol.* **11,** 1392–1402
13. de Wit, H., Lichtenstein, Y., Kelly, R. B., Geuze, H. J., Klumperman, J., and van der Sluijs, P. (2001) *Mol. Biol. Cell* **12,** 3703–3715
14. van der Sluijs, P., Hull, M., Zahraoui, A., Tavitian, A., Goud, B., and Mellman, I. (1991) *Proc. Natl. Acad. Sci. U. S. A.* **88,** 6313–6317
15. de Wit, H., Lichtenstein, Y., Geuze, H., Kelly, R. B., van der Sluijs, P., and Klumperman, J. (1999) *Mol. Biol. Cell* **10,** 4163–4176
16. Bailly, E., Touchot, N., Zahraoui, A., Goud, B., and Bornens, M. (1991) *Nature* **350,** 715–718
17. van der Sluijs, P., Hull, M., Huber, L. A., Male, P., Goud, B., and Mellman, I. (1992) *EMBO J.* **11,** 4379–4389
18. Gerez, L., Mohrmann, K., van Raak, M., Jongeneelen, M., Zhou, X. Z., Lu, K. P., and van der Sluijs, P. (2000) *Mol. Biol. Cell* **11,** 2201–2211
19. Nagelkerken, B., Mohrmann, K., Gerez, L., van Raak, M., Leijendekker, R. L., and van der Sluijs, P. (1997) *Electrophoresis* **18,** 2694–2698
20. Galli, T., Chilcote, T., Mundigl, O., Binz, T., Niemann, H., and De Camilli, P. (1994) *J. Cell Biol.* **125,** 1015–1024
21. Bottger, G., Nagelkerken, B., and van der Sluijs, P. (1996) *J. Biol. Chem.* **271,** 29191–29197
22. Evan, G. I., Lewis, G. K., Ramsay, G., and Bishop, J. M. (1985) *Mol. Cell. Biol.* **5,** 3610–3616
23. Kreis, T. E. (1987) *EMBO J.* **6,** 2597–2606
24. Daro, E., van der Sluijs, P., Galli, T., and Mellman, I. (1996) *Proc. Natl. Acad. Sci. U. S. A.* **93,** 9559–9564
25. Sprong, H., Kruithof, B., Leijendekker, R., Slot, J. W., van Meer, G., and van der Sluijs, P. (1998) *J. Biol. Chem.* **273,** 25880–25888
26. Gorvel, J. P., Chavrier, P., Zerial, M., and Gruenberg, J. (1991) *Cell* **64,** 915–925
27. Van Weert, A., Dunn, K. W., Geuze, H. J., Maxfield, F. R., and Stoorvogel, W. (1995) *J. Cell Biol.* **130,** 821–834
28. Geuze, H. J., Slot, J. W., van der Ley, P., Scheffer, R. T. C., and Griffith, J. W. (1981) *J. Cell Biol.* **89,** 653–665
29. Slot, J. W., Geuze, H. J., Gigenack, S., Lienhard, G. E., and James, D. E. (1991) *J. Cell Biol.* **113,** 123–125
30. Liou, W., Geuze, H. J., Geelen, M. J. H., and Slot, J. W. (1997) *J. Cell Biol.* **136,** 61–70
31. Sprong, H., Degroote, S., Claessens, T., van Drunen, J., Oorschot, V., Westerink, B. H. C., Hirabayashi, Y., Klumperman, J., van der Sluijs, P., and van Meer, G. (2001) *J. Cell Biol.* **155,** 369–379
32. Ayad, N., Hull, M., and Mellman, I. (1997) *EMBO J.* **16,** 4497–4507
33. Soldati, T., Shapiro, A. D., Svejstrup, A. B. D., and Pfeffer, S. (1994) *Nature* **369,** 76–78
34. Ullrich, O., Horiuchi, H., Bucci, C., and Zerial, M. (1994) *Nature* **368,** 157–160
35. Annaert, W. G., Becker, B., Kistner, U., Reth, M., and Jahn, R. (1997) *J. Cell Biol.* **139,** 1397–1410
36. Klumperman, J., Schweizer, A., Clausen, H., Tang, B. L., Hong, W., Oorschot, V., and Hauri, H. P. (1998) *J. Cell Sci.* **111,** 3411–3425
37. Futter, C. E., Gibson, A., Allchin, E. H., Maxwell, S., Ruddock, L. J., Odorizzi, G., Domingo, D., Trowbridge, I. S., and Hopkins, C. R. (1998) *J. Cell Biol.* **141,** 611–624
38. Mohrmann, K., Leijendekker, R., Gerez, L., and van der Sluijs, P. (2002) *J. Biol. Chem.* **277,** 10474–10481
39. Bourne, H. R. (1988) *Cell* **53,** 669–671
40. Brennwald, P. (2000) *J. Cell Biol.* **149,** 1–3
41. Nuoffer, C., Davidson, H., Matteson, J., Meinkoth, J., and Balch, W. E. (1994) *J. Cell Biol.* **125,** 225–238
42. McLaughlan, H., Newell, J., Morrice, N., Osborne, A., West, M., and Smythe, E. (1998) *Curr. Biol.* **8,** 34–45
43. Carroll, K. S., Hanna, J., Simon, I., Krise, J., Barbero, P., and Pfeffer, S. R. (2001) *Science* **292,** 1373–1376
44. Segev, N., Mullholland, J., and Botstein, D. (1988) *Cell* **52,** 915–924
45. Salminen, A., and Novick, P. J. (1987) *Cell* **49,** 527–538
46. Horazdovski, B. F., Busch, G. R., and Emr, S. (1994) *EMBO J.* **13,** 1297–1309
47. Wu, X. S., Rao, K., Zhang, H., Sellers, J. R., Matesic, L. E., Copeland, N. G., Jenkins, N. A., and Hammer, J. A., III (2002) *Nat. Cell Biol.* **4,** 1–8
48. Haddad, E. K., Wu, X., Hammer, J. A., III, and Henkart, P. A. (2001) *J. Cell Biol.* **152,** 835–842
49. Nagelkerken, B., van Anken, E., van Raak, M., Gerez, L., Mohrmann, K., van Uden, N., Holthuizen, J., Pelkmans, L., and van der Sluijs, P. (2000) *Biochem. J.* **346,** 593–601
50. Vitale, G., Rybin, V., Christoforidis, S., Thornqvist, P. O., McCaffrey, M., Stenmark, H., and Zerial, M. (1998) *EMBO J.* **17,** 1941–1951
51. de Renzis, S., Sönnichsen, B., and Zerial, M. (2002) *Nat. Cell Biol.* **4,** 124–133
52. Cormont, M., Mari, M., Galmiche, A., Hofman, P., and Le Marchand-Brustel, Y. (2001) *Proc. Natl. Acad. Sci. U. S. A.* **98,** 1637–1642
53. Bielli, A., Thörnqvist, P. O., Hendrick, A. G., Finn, R., Fitzgerald, K., and McCaffrey, M. W. (2001) *Biochem. Biophys. Res. Commun.* **281,** 1141–1153

rab4 Function in Membrane Recycling from Early Endosomes Depends on a Membrane to Cytoplasm Cycle

Karin Mohrmann, Lisya Gerez, Viola Oorschot, Judith Klumperman and Peter van der Sluijs

Access the most updated version of this article at doi: 10.1074/jbc.M203064200

Alerts:
- When this article is cited
- When a correction for this article is posted

Click here to choose from all of JBC's e-mail alerts

This article cites 53 references, 29 of which can be accessed free at
http://www.jbc.org/content/277/35/32029.full.html#ref-list-1